Standard Operating Procedure for collection, evaluation and histological grading of lungs for research studies

I. Recommended Materials

Dissecting board with cork or rubber surface
Spray bottle loaded with 70% Ethanol
Pins (to tack down carcass, user preference)
Forceps
Scalpel blade or other sharp blade
2 scissors (one for removing the rib cage, the second dedicated for soft tissue dissection)
3cc syringe with 21g needle
10% neutral buffered formalin (at least 25mL to maintain recommended 15-20:1 volume:tissue ratio)
Permanent marker for labeling
Metric scale

II. Procedure

In most instances, it is understood that the necropsy procedure and collection of lung tissue will be only a portion of a detailed postmortem examination involving observation and collection of all major organ systems. For the purposes of this standard operating procedure, details will be restricted to collection and examination of lung tissue only.

Prior to beginning necropsy, obtain body weight of murine subject. Label tube or other sealed vessel that contains 10% neutral buffered formalin with all identification parameters available (minimum data base would include mouse identification number, mouse strain, weight, research study and date)

1. Secure mouse to dissecting board using tacks or pins. The mouse is positioned in dorsal recumbency with full extension of pelvic and pectoral limbs
2. Soak/wet the carcass with 70% ethanol using spray bottle
3. Using forceps, grasp the skin over the sternum and make an initial incision at the ventral midline. Continue the incision cranially/caudally along the ventral midline to extend from the chin to the pubis.
4. From the ventral midline incision, gently reflect the skin bilaterally from the ventral thorax and abdomen completing exposing the subcutis of the ventral and lateral thorax and abdomen.
5. Make a ventral midline incision into the abdomen to expose the peritoneal cavity and to expose the xiphoid process
6. Grasp the xiphoid process with forceps and use scissors (the scissors dedicated to removing the rib cage) to cut the ribs on each side of the sternum at about the mid-level of the body of the ribs. Retract the xiphoid cranially as the ribs are cut, extending the cuts on both sides to the thoracic inlet. Subsequently, the rib cage will be removed and the entire thoracic cavity exposed.
7. Remove the tongue by cutting the mandibular symphysis with scissors and retracting the tongue caudally with forceps.

8. While grasping the tongue with forceps and retracting caudally, cut all dorsal attachments with scissors removing the tongue, esophagus, trachea, heart and lungs en bloc. The esophagus is the dorsal landmark through the cervical region. The aorta is the dorsal landmark in the thoracic cavity (ie. the aorta is removed with the heart/lungs.
9. Perform gross examination of pulmonary tissue and record findings.
10. Using 3-5cc syringe and 25 or 27g needle, gently thread needle into trachea, clasp outside of trachea with forceps to hold needle in place, and gently inflate lungs with formalin until they are fully expanded to normal level as expected to fill the chest cavity (Take care not to over- or under-inflate the lung).
11. Drop en bloc organ mass, including the lungs in formalin
12. Special considerations

a. Organ weights-lung weights can be obtained at any time before formalin infusions. The lung mass can be removed from the en bloc sample by transection of the distal trachea just cranial to the tracheal bifurcation.

b. Inflation of lungs with formalin is critical prequel to histological assessment. Under- or non-inflated lungs impair evaluation of alveolar septa

c. Depending upon the study, evaluation of the alveolar septa may be critical such that inflation of lungs must be accurately consistent and/or alveolar septal capillaries are required to be cleared of remaining blood

i. To clear lungs of blood, insert needle into the right ventricle of the heart and gently instill formalin. The lungs will slightly inflate and transition from red/pink to completely white when completed.

ii. More consistent infusion of lungs can be obtained by slightly more complicated methods that typically require more time, equipment and expertise. These are outlined in reference 3. It should be noted that "eyeball" infusion of lungs with formalin through the trachea is acceptable and generally considered the best procedure.

References

1. Knoblaugh S, Randolph-Habecker J, Rath, S. Necropsy and Histology. IN: Comparative anatomy and histology: a mouse and human atlas. Eds Treuting P and Dintzis S. Academic Press, Waltham, MA USA, 2012.

2. Renne R, Fouillet X, Maurer J, Assaad A, Morgan K, Hahn F, Nikula K, Gillet N, Copley N. Recommendation of optimal method for formalin fixation of rodent lungs in routine toxicological studies. Toxicol Pathol 29:587-589, 2001.

3. Braber S, Verheijden K, Henricks P, Kraneveld A, Folkerts G. A comparison of fixation methods on lung morphology in a murine model for emphysema. Am J Physiol Lung Cell Mol Physiol 299: L843-851, 2010.

III. Post-fixation dissection.

Post fixation dissection or preparation of tissues for heat processing, paraffin embedded tissue sectioning is arguably one of the most important steps of the lung evaluation procedure. Standardized trimming of tissues is needed in research studies to maintain consistency in organ sampling across individual mice (1). Notes and observations made during the gross examination should always be available and referenced during post-fixation dissection.

In most instances, the size of the entire murine lung mass is amenable to histological evaluation in toto. Exceptions would include either very large lesions that may not fit with the remainder of the lung or very small lesions that may otherwise be missed during sectioning. Histological evaluation should

include: 1) any grossly observed lesions and 2) in toto lung mass and 3) distal trachea with peri-tracheal/mediastinal connective tissue containing lymph nodes.

Method

1. Lungs lobes (5) can be placed in toto in tissue cassette, ventral side down
    a) left lung lobe
    b) right cranial lung lobe
    c) right middle lung lobe
    d)right caudal lung lobe
    e) accessory lung lobe

2. Histological sectioning would proceed longitudinally and horizontally
3. Judgement call is made as to whether grossly observed lesions would be missed from in toto sectioning. If so, particular lesion is isolated (based upon gross observations), sectioned and placed in cassette. However, remaining lung tissue is placed in cassette and oriented (ventral side down) in toto.
4. Distal trachea and peri-tracheal connective tissue is placed in same (if room) or different cassette (if no room).

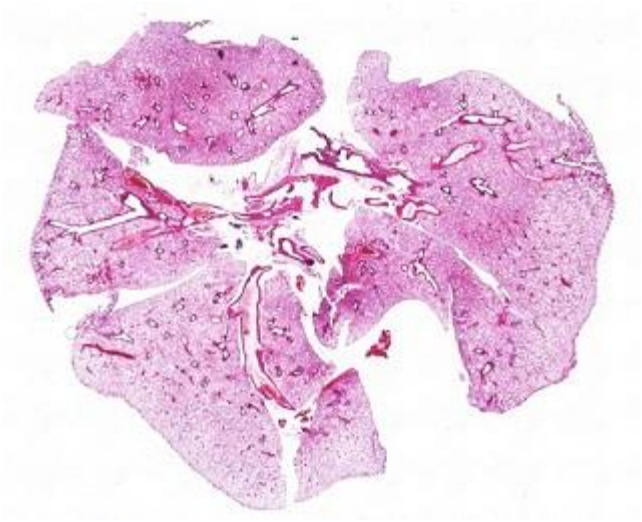

From:
http://reni.item.fraunhofer.de/reni/trimming/index.php

Considerations

In toto lung sectioning provides complete look across hilar and peripheral lung regions for any possible lesions. In most cases, grossly observed lesions will be present following sectioning of *in toto* lungs. Exceptions might include tiny/small, peripherally placed lesions that might be removed during block face-in. For this reason, some lesions (whether big or small) may need to be isolated and embedded individually. It is critically important to include lymph nodes for histological evaluation. These are especially important for determining extension of neoplastic disease (metastasis) as a criterion for malignancy during evaluation of lung tumors.

References

4. Kittel B, Ruehl-Fehlert C, Morawietz G, Klapwijk J, Elwell M, Lenz B, O'Sullivan G, Roth D, Wadsworth P. Revised guides for organ sampling and trimming in rats and mice-Part 2: a joint publication of the RITA and NACAD groups. Exp Toxicol Pathol 55:413-431, 2004.

5. User interactive and searchable webpage of recommendations from Reference 4 can be found at: http://reni.item.fraunhofer.de/reni/trimming/index.php

IV. Histological Evaluation

A. Scoring inflammatory lesions

According to a review by Klopfleisch, there are 14 original semiquantitative, multiparametric scoring systems identified for pulmonary diseases. Most addressed pulmonary fibrosis and inflammation. Most scoring systems for lung inflammation address either acute inflammation or inflammation secondary to models of infectious disease (Pneumocystis, Mycoplasma, Streptococcus, etc.) and these may not (and probably are not) applicable to inflammation expected in aging mice.

1. A subjective scoring system originally adapted for acute lung injury (ALI) and proposed by the American Thoracic Society includes assessment of features of inflammation in both air spaces and interstitium, but does not necessarily identify anatomic location. A modification of this grading system could be useful if inflammatory cells were broadened to include particularly lymphocytes and macrophages, which are more likely to be found in chronic inflammation in aging mice. Still, retention of some of the acute factors of this grading scale (neutrophils, hyaline membranes, etc). would allow identification of this type of injury if present.

TABLE 1. LUNG INJURY SCORING SYSTEM

	Score per field		
Parameter	0	1	2
A. Neutrophils in the alveolar space	none	1–5	>5
B. Neutrophils in the interstitial space	none	1–5	>5
C. Hyaline membranes	none	1	>1
D. Proteinaceous debris filling the airspaces	none	1	>1
E. Alveolar septal thickening	<2x	2x–4x	>4x

$$\text{Score} = [(20 \times A) + (14 \times B) + (7 \times C) + (7 \times D) + (2 \times E)]/(\text{number of fields} \times 100)$$

(Table 1 from Reference 7)

2. Inflammation can be separated based upon the two major, classical pattern recognition of pulmonary injury, either airway or interstitial disease. Bronchointerstitial pneumonias, if present, would be grouped with airway disease based upon pathogenesis indicating airway entry of disease. Once separated, the airway or interstitial inflammation would be graded as normal to mild, moderate, severe (0-4 on numerical scale) or graded according to pre-existing scoring models (8,9 for example). Some of these scoring models could also take into account other changes that accompany inflammation, such as airway hyperplasia, that may also be important to correlate with proliferative or neoplastic disease.

3. Similar to as proposed for scoring of fibrosis below, inflammation could simply be scored based upon the percent or area of total lung area occupied by inflammation. Although the type or character of the inflammation could be noted, this system simply records percent lung involvement as it may relate to functional parameters.

4. An optimal method for quantitative assessment of lung inflammation would be to follow the protocol as outlined by Apfeldorfer et al. (10). Although this grading procedure is technologically more complicated, it provides a more quantitative assessment. It requires that addition of immunofluorescent markers to quantitate inflammatory cells and products, digital slide scanner/acquisition technology and analysis (morphometric type) software.

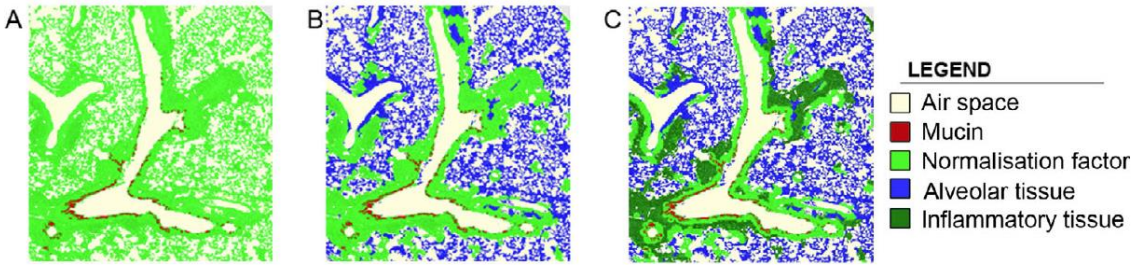

References

6. Klopfleisch R. Multiparametric and semiquantitative scoring systems for the evaluation of mouse model histopathology-a systematic review. BMC Vet Res 9:123-138, 2013.

7. Matute-Bello G, Downey G, Moore BB, Groshong SD, Matthay MA, Slutsky AS, Kuebler WM. An Official American Throacic Society Workshop Report: Features and measurements of experimental acute lung injury in animal. Am J Respir Cell Mol Biol 44:725-738, 2011.

8. Pinson DM, Schoeb TR, Lindsey JR, Davis JK. Evaluation by scoring and computerized morphometry of lesions of early Mycoplasma pulmonis infection and ammonia exposure in F344/N rats. Vet Pathol 23:550-555, 1986.

9. Germann PG, Hafner D. A rat model of acute respiratory distress syndrome (ARDS): Part 1. Time dependency of histological and pathological changes. J Pharmacol Toxicol Methods 40: 101-107, 1998.

10. Apfeldorfer C, Ulrich K, Jones G, Goodwin D, Collins S, Schenck E, Richard V. Object oriented automated image analysis: quantitative and qualitative estimation of inflammation in mouse lung. Diagn Pathol 3 (Suppl): S1-S16, 2008.

B. Scoring fibrotic lesions

There are several histological scoring methods for pulmonary fibrosis; most either use or are derived from a numerical scale method introduced by Ashcroft et al. (11) While useful, the Ashcroft scale has some drawbacks, which are outlined in (12). Hubner et al. improved the Ashcroft scale by modifications resulting in high intra-observer agreement and a higher correlation of the histological score with CT scans indicating the modified scale is reliable and reproducible.

Scoring fibrotic lesions can proceed in one of two formats

1. Fibrotic lesions are scored by method of Hubner et al as outlined in Table below (from Hubner, Reference 12). All histological specimens for scoring are stained with Masson's Trichrome to highlight connective tissue deposition.

Table 2. Characterization of the Modified Scale

Grade of Fibrosis	Sample Photograph	Modified Scale
0	Figure 1A	**Alveolar septa**: No fibrotic burden at the most flimsy small fibers in some alveolar walls **Lung structure**: Normal lung
1	Figure 1B	**Alveolar septa**: Isolated gentle fibrotic changes (septum ≤3× thicker than normal) **Lung structure**: Alveoli partly enlarged and rarefied, but no fibrotic masses present
2	Figure 1C	**Alveolar septa**: Clearly fibrotic changes (septum >3× thicker than normal) with knot-like formation but not connected to each other **Lung structure**: Alveoli partly enlarged and rarefied, but no fibrotic masses
3	Figure 1D	**Alveolar septa**: Contiguous fibrotic walls (septum >3× thicker than normal) predominantly in whole microscopic field **Lung structure**: Alveoli partly enlarged and rarefied, but no fibrotic masses
4	Figure 1E	**Alveolar septa**: Variable **Lung structure**: Single fibrotic masses (≤10% of microscopic field)
5	Figure 1F	**Alveolar septa**: Variable **Lung structure**: Confluent fibrotic masses (>10% and ≤50% of microscopic field). Lung structure severely damaged but still preserved
6	Figure 1G	**Alveolar septa**: Variable, mostly not existent **Lung structure**: Large contiguous fibrotic masses (>50% of microscopic field). Lung architecture mostly not preserved
7	Figure 1H	**Alveolar septa**: Non-existent **Lung structure**: Alveoli nearly obliterated with fibrous masses but still up to five air bubbles
8	Figure 1I	**Alveolar septa**: Non-existent **Lung structure**: Microscopic field with complete obliteration with fibrotic masses

2. Quantitative assessment of fibrotic lesions

Utilizing the method outline by Hubner et al is simple and supposedly reliable and reproducible. Utilizing the Masson's Trichrome and digital capture technology, it is possible to assign the color of fibrosis (blue) in the Trichrome and convert to binary image. This results in image where everything blue is black and everything not blue is colorless. From this, using software (such as NIH Image J), the pixels that are black (or blue on the Trichrome) can be quantitated and reported as a percent of the section. The end result would be a % increase or decrease in deposition or % of total area occupied by collagen in the sample that could be compared between animals or against control (younger animals).

For example, I recently quantitated glycogen* in the right and left auricular appendage of goats and dogs using a PAS stain (with and without diastase digestion). Glycogen in the PAS stains is red/purple and is converted to black in the binary image. The amount of glycogen in the image compared to total area is automatically calculated by the software resulting in a fairly objective value.

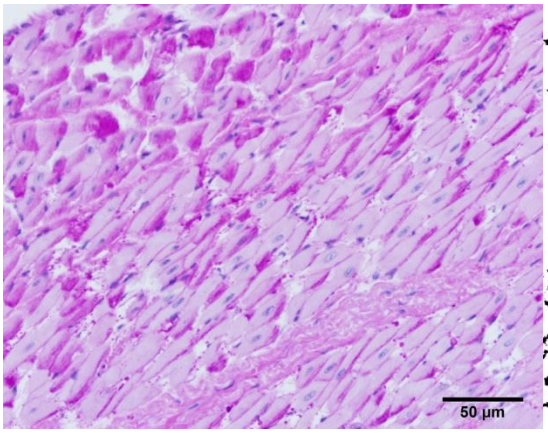

Panel A. PAS stain demonstrating glycogen within cardiac myocytes

Panel B. Image in Panel A converted to binary image.

*Embi AA, Scherlag BJ, Ritchey JW. Glycogen and the propensity for atrial fibrillation: intrinsic anatomic differences in glycogen in the left and right atria in the goat heart. N Am J Med Sci 6:510-515, 2014.

In summary, this or a similar method could easily be employed to measure and score fibrotic lesions in murine pulmonary tissues.

References

11. Ashcroft T, Simpson JM, Timbrell V. Simple method of estimating severity of pulmonary fibrosis on a numerical scale. J Clin Pathol 41: 467-470, 1988.

12. Hubner RH, Gitter W, El Mokhtari NE, Mathiak M, Both M, Bolte H, Freitag-Wolf S, Bewig B. Standardized quantification of pulmonary fibrosis in histological samples. Biotechniques 44: 507-517, 2008.

C. Classification of proliferative and neoplastic lesions

Classification of hyperplastic and neoplastic lesions will follow metrics as previously published by Nikitin et al. Classification metric tabulated below (Table 3 taken from Reference 13)

Table 3 *Classification of the proliferative pulmonary lesions of the mouse*[a]

1. Epithelial
1.1. Hyperplasia
1.1.1. Epithelial
1.1.1.1. Airways
1.1.1.2. Alveoli
1.1.2. Neuroendocrine

1.2. Tumors
1.2.1. Benign
1.2.1.1. Papilloma
1.2.1.2. Adenoma
1.2.1.2.1. Solid
1.2.1.2.2. Papillary
1.2.1.2.3. Mixed subtypes
1.2.2. Preinvasive lesions
1.2.2.1. Squamous dysplasia
1.2.2.2. Atypical adenomatous hyperplasia
1.2.2.3. Diffuse pulmonary neuroendocrine cell hyperplasia
1.2.3. Malignant
1.2.3.1. Squamous cell carcinoma
1.2.3.2. Adenocarcinoma
1.2.3.2.1. Papillary
1.2.3.2.2. Acinar
1.2.3.2.3. Solid
1.2.3.2.4. Mixed subtypes
1.2.3.2.5. NOS
1.2.3.3. Adenosquamous carcinoma
1.2.3.4. Neuroendocrine carcinoma
1.2.3.5. Carcinoma, other
2. Soft tissue
3. Mesothelial
4. Miscellaneous
5. Lymphoproliferative
6. Secondary
7. Unclassified
8. Tumor-like lesions

[a] Modifiers should be used when sufficient information is available on the location and cell origin of the lesions, including Clara cell, type II pneumocyte, and so forth

References

13. Nikitin AY, Alcaraz A, Anver MR, Bronson RT, Cardiff RD, Dixon D, Fraire AE, Gabrielson EW, Gunning WT, Haines DC, Kaufman MH, Linnoila RI, Maronpot RR, Rabson AS, Reddick RL, Rehm S, Rozengurt N, Schuller HM, Shmidt EN, Travis WD, Ward JM, Jacks T. Classification of proliferative pulmonary lesions of the mouse: recommendations of the mouse models of human cancers consortium. Cancer Res 64:2307-2317, 2004.

Complete Bibiliography

Aoshiba K, Nagai A. Chronic lung inflammation in aging mice. FEBS Letters 581:3512-3516, 2007.

Apfeldorfer C, Ulrich K, Jones G, Goodwin D, Collins S, Schenck E, Richard V. Object oriented automated image analysis: quantitative and qualitative estimation of inflammation in mouse lung. Diagn Pathol 3 (Suppl): S1-S16, 2008.

Ashcroft T, Simpson JM, Timbrell V. Simple method of estimating severity of pulmonary fibrosis on a numerical scale. J Clin Pathol 41: 467-470, 1988.

Brayton CF, Treuting PM, Ward JM. Pathobiology of aging mice and GEM: Background strains and experimental design. Vet Pathol 49:85-105, 2012.

Bregman CL, Adler RR, Morton DG, Regan KS, Yano BL. Recommended tissue list for histopathologic examination in repeat-dose toxicity and carcinogenicity studies: a proposal of the society of toxicological pathology (STP). Toxicol Pathol 31: 252-253, 2003.

Curtis JL, Warnock ML, Arraj SM, Kaltreider HB. Histologic analysis of an immune response in the lung parenchyma of mice: angiopathy accompanies inflammatory cell influx. Am J Pathol 137:689-699, 1990.

Dungworth DL, Rittinghausen S, Schwartz L, Harkema JR, Hayashi Y, Kittel B, Lewis D, Miller RA, Mohr U, Morgan KT, Rehm S, Slayter MV. Respiratory System and Mesothelium. IN:International Classification of rodent tumors: the mouse. ED: Mohr U. Springer, New York, NY USA, 2001.

Germann PG, Hafner D. A rat model of acute respiratory distress syndrome (ARDS): Part 1. Time dependency of histological and pathological changes. J Pharmacol Toxicol Methods 40: 101-107, 1998.

Gibson-Corley KN, Olivier AK, Meyerholz DK. Principles for valid histopathologic scoring in research. Vet Pathol 50:1007-1015, 2013.

Haines DC, Chattopadhyay S, Ward JM. Pathology of aging B6;129 mice. Toxicol Pathol 29:653-661, 2001.

Holland T, Holland C. Analysis of unbiased histopathology data from rodent toxicity studies (or, are these groups different enough to ascribe it to treatment?). Toxicol Pathol 39:569-575, 2011.

Hubner RH, Gitter W, El Mokhtari NE, Mathiak M, Both M, Bolte H, Freitag-Wolf S, Bewig B. Standardized quantification of pulmonary fibrosis in histological samples. Biotechniques 44: 507-517, 2008.

Klopfleisch R. Multiparametric and semiquantitative scoring systems for the evaluation of mouse model histopathology-a systematic review. BMC Vet Res 9:123-138, 2013.

Knoblaugh S, Randolph-Habecker J, Rath, S. Necropsy and Histology. IN: Comparative anatomy and histology: a mouse and human atlas. Eds Treuting P and Dintzis S. Academic Press, Waltham, MA USA, 2012.

Lawson WE, POlosukhin VV, Stathopoulos GT, Zoia O, Han W, Lane KB, Li B, Donnelly EF, Holburn GE, Lewis KG, Collins RD, Hull WM, Glasser SW, Whitsett JA, Blackwell TS. Increased and prolonged pulmonary fibrosis in surfactant protein C-deficient mice following intratracheal bleomycin. Am J Pathol 167:1267-1277, 2005.

Matute-Bello G, Downey G, Moore BB, Groshong SD, Matthay MA, Slutsky AS, Kuebler WM. An Official American Throacic Society Workshop Report: Features and measurements of experimental acute lung injury in animal. Am J Respir Cell Mol Biol 44:725-738, 2011.

Morton D, Kemp RK, Francke-Carroll S, Jensen K, McCartney J, Monticello TM, Perry R, Pulido O, Roome N, Schafer K, Sellers R, Snyder PW. Best practices for reporting pathology interprestations within GLP toxicology studies. Toxicol Pathol 34:806-809, 2006.

Nikitin AY, Alcaraz A, Anver MR, Bronson RT, Cardiff RD, Dixon D, Fraire AE, Gabrielson EW, Gunning WT, Haines DC, Kaufman MH, Linnoila RI, Maronpot RR, Rabson AS, Reddick RL, Rehm S, Rozengurt N,

Pettan-Brewer C, Treuting PM. Practical pathology of aging mice. Pathobiol Aging Age Relat Dis. 2011;1. doi: 10.3402/pba.v1i0.7202. Epub 2011 Jun 1.

Pinson DM, Schoeb TR, Lindsey JR, Davis JK. Evaluation by scoring and computerized morphometry of lesions of early Mycoplasma pulmonis infection and ammonia exposure in F344/N rats. Vet Pathol 23:550-555, 1986.

Schuller HM, Shmidt EN, Travis WD, Ward JM, Jacks T. Classification of proliferative pulmonary lesions of the mouse: recommendations of the mouse models of human cancers consortium. Cancer Res 64:2307-2317, 2004.

Sellers RS, Morton D, Michael B, Roome N, Johnson JK, Yano BL, Perry R, Schafer K. Society of Toxicologic Pathology position paper: organ weight recommendations for toxicology studies. Toxicol Pathol 35:751-755, 2007.

Wakamatsu N, Devereux TR, Hong HH, Sills RC. Overview of the molecular carcinogenesis of mouse lung tumor models of human lung cancer. Toxicol Pathol 35:75-80, 2007.